ARTICLE
Journal of Cellular Biochemistry 116:648–660 (2015)

Journal of Cellular Biochemistry

Regulation of Mitochondrial Morphology by Positive Feedback Interaction Between PKCδ and Drp1 in Vascular Smooth Muscle Cell

Soyeon Lim,[1] Se-Yeon Lee,[2] Hyang-Hee Seo,[2] Onju Ham,[2] Changyeon Lee,[3] Jun-Hee Park,[3,4] Jiyun Lee,[2] Minji Seung,[2] Ina Yun,[2] Sun M. Han,[2] Seahyoung Lee,[4,5] Eunhyun Choi,[4,5] and Ki-Chul Hwang[4,5]*

[1]*Severance Integrative Research Institute for Cerebral & Cardiovascular Disease, Yonsei University Health System, Seodaemun-gu, Seoul 120-752, Republic of Korea*

[2]*Brain Korea 21 Project for Medical Science, Yonsei University College of Medicine, Seodaemun-gu, Seoul 120-752, Republic of Korea*

[3]*Department of Integrated Omics for Biomedical Sciences, Graduate School, Yonsei University, Seodaemun-gu, Seoul 120-749, Republic of Korea*

[4]*Catholic Kwandong University, International St. Mary's Hospital, Incheon Metropolitan City, 404-834, Republic of Korea*

[5]*Institute for Bio-Medical Convergence, College of Medicine, Catholic Kwandong University, Gangneung-si, Gangwon-do 210-701, Republic of Korea*

ABSTRACT

Dynamin-related protein-1 (Drp1) plays a critical role in mitochondrial fission which allows cell proliferation and Mdivi-1, a specific small molecule Drp1 inhibitor, is revealed to attenuate proliferation. However, few molecular mechanisms-related to Drp1 under stimulus for restenosis or atherosclerosis have been investigated in vascular smooth muscle cells (vSMCs). Therefore, we hypothesized that Drp1 inhibition can prevent vascular restenosis and investigated its regulatory mechanism. Angiotensin II (Ang II) or hydrogen peroxide (H_2O_2)-induced proliferation and migration in SMCs were attenuated by down-regulation of Drp1 Ser 616 phosphorylation, which was demonstrated by in vitro assays for migration and proliferation. Excessive amounts of ROS production and changes in mitochondrial membrane potential were prevented by Drp1 inhibition under Ang II and H_2O_2. Under the Ang II stimulation, activated Drp1 interacted with PKCδ and then activated MEK1/2-ERK1/2 signaling cascade and MMP2, but not MMP9. Furthermore, in ex vivo aortic ring assay, inhibition of the Drp1 had significant anti-proliferative and -migration effects for vSMCs. A formation of vascular neointima in response to a rat carotid artery balloon injury was prevented by Drp1 inhibition, which shows a beneficial effect of Drp1 regulation in the pathologic vascular condition. Drp1-mediated SMC proliferation and migration can be prevented by mitochondrial division inhibitor (Mdivi-1) in in vitro, ex vivo and in vivo, and these results suggest the possibility that Drp1 can be a new therapeutic target for restenosis or atherosclerosis. J. Cell. Biochem. 116: 648–660, 2015.

KEY WORDS: VASCULAR SMOOTH MUSCLE CELL; NEOINTIMAL FORMATION; PROLIFERATION; MIGRATION; Drp1; PKCδ

S. Lim, S. Y. Lee and H. H. Seo contributed equally to this work.

Grant sponsor: Korea Science and Engineering Foundation Grant funded by the Korean Government (MEST); Grant number: 2014030459; Grant sponsor: Korean Health Technology R&D Project, Ministry of Health & Welfare, Republic of Korea; Grant number: A120478; Grant sponsor: Yonsei University College of Medicine for 2013; Grant number: 2013-32-0051; Grant sponsor: Korea Health 21 R&D Project, Ministry of Health & Welfare, Republic of Korea; Grant number: HI08C2149.

*Correspondence to: Prof. Ki-Chul Hwang, PhD, Institute for Bio-Medical Convergence, College of Medicine, Catholic Kwandong University, Gangneung-si, Gangwon-do, 210-701, Republic of Korea. E-mail: kchwang@cku.ac.kr

Manuscript Received: 27 August 2014; Manuscript Accepted: 28 October 2014

Accepted manuscript online in Wiley Online Library (wileyonlinelibrary.com): 16 November 2014

DOI 10.1002/jcb.25016 • © 2014 Wiley Periodicals, Inc.

The proliferation and migration of vascular smooth muscle cells (vSMCs) are critical events during cardiovascular remodeling such as restenosis after angioplasty [Zempo et al., 1996], which is generally accepted to contribute to neointimal formation [Hehrlein et al., 1995]. During this process, vSMCs initially migrate into intima after the endothelial destruction [Schwartz et al., 1995], proliferation is then stimulated by growth factors and hormones such as transforming growth factor-β1 (TGF-β1), tumor necrosis factor-alpha (TNF-α), or Angiotensin II (Ang II) for a period of weeks to months [Tanaka et al., 1996; Jandeleit-Dahm et al., 1997; Khan et al., 2007]. Therefore, there have been many efforts to inhibit the proliferation and migration of vSMCs by blocking receptors and regulating cytokines related to the cell cycle using a variety of methods, including medical devices and pharmaceutical agents [Banai et al., 1998; Yamada et al., 2007]. Nevertheless, restenosis still occurs in 10% of patients [Farooq et al., 2011].

In aortic stenosis and coronary atherosclerotic plaques, the role of Ang II is well determined related to vSMCs as well as other inflammatory cells [Schieffer et al., 2000; Rajamannan, 2009]. Function of Ang II in cardiovascular cells has been known to work through Angiotensin II type 1 receptor (AT1R) whose activation increases reactive oxygen species (ROS), resulting in vSMCs proliferation and migration in a vital dose [Zhang et al., 2007]. AT1R is known to produce ROS from NAD(P)H oxidases (Nox) activation through PKC activation, where ROS activates Src to further generate ROS through EGFR transactivation and GTP-bound Rac generation [Seshiah et al., 2002].

Mitochondria are dynamic, multi-tasking organs that play pivotal roles in the cell survival and death of a variety of cell types by ATP production, calcium handling, and ROS production [Brookes et al., 2004]. In addition, mitochondria regulate proliferation by altering their shape and movement depending on various stimuli; this phenomenon has been investigated in proliferating vSMCs [Chalmers et al., 2012]. Various cytosolic and mitochondrial proteins play roles in this dynamic process, which has been studied in cardiovascular diseases and cancer. Mitochondrial fission (fragmentation) and fusion (interconnection) are very important for regulating the cell cycle. The GTPase dynamin-related protein 1 (Drp1) promotes mitochondrial fission, and GTPase mitofusion 1 and 2 (Mfn1/2) are responsible for fusion [Westermann, 2010]. Drp1 is mainly located in cytosol; upon activation by a stimulus, it moves to the mitochondrial outer membrane and binds to a mitochondrial outer membrane protein (hFis1) to exert its effects [Yu et al., 2005]. Cyclin B1/cyclin-dependent kinase 1 (CDK1) was reported to phosphorylate Drp1 at Ser 585 or Ser‘ 616 in Hela cells or lung cancer cells [Taguchi et al., 2007; Rehman et al., 2012]. Interestingly, a recent study showed that the phosphorylation of Drp1 at the different sites regulated its function in an opposing manner. Specifically, phosphorylation at Ser-616 by CDK1 enhanced Drp1 activity, whereas phosphorylation at Ser-637 by PKA inhibited Drp1 activity [Rehman et al., 2012]. It was recently reported that protein kinase C-delta (PKCδ) could activate Drp1 at Ser-579/616. Moreover, PKCδ and Drp1 translocate into mitochondria as a complex, which increases fission; these two proteins have an interdependent relationship in human neuronal cells [Qi et al., 2011].

Mdivi-1 is an inhibitor of mitochondrial division and mitophagy that functions as a Drp1-specific inhibitor. Studies over the last 2 years have assessed the inhibitory effect of Mdivi-1 on Drp1 in cardiovascular diseases. Data revealed that Mdivi-1 treatment exerted protective effects on cardiac cell death and pulmonary SMC hyperproliferation during doxorubicin-induced cardiotoxicity [Gharanei et al., 2013], pressure overload induced heart failure [Givvimani et al., 2012], ischemia-reperfusion injury [Sharp et al., 2014], and pulmonary hypertension [Marsboom et al., 2012b]. Mdivi-1 also protected against ductus arteriosus by inhibiting ductal SMCs [Hong et al., 2013]. Nevertheless, the role of Drp1 in vSMCs during restenosis and related signaling pathways that regulate the effects of PKCδ/Drp1 on proliferation and migration are poorly understood.

In this study, we tested the hypothesis that Drp1-specific inhibition attenuates vSMC proliferation and migration, and investigated the regulatory mechanisms of Drp1, as well as its interaction with other signaling molecules during restenosis-induced or atherosclerotic stimuli.

MATERIALS AND METHODS

ETHICS STATEMENT

All experimental procedures of our animal studies were approved by the Institutional Animal Care and Use Committee (IACUC, approval No. 2012–0197) at Yonsei University College of Medicine and were performed in accordance with the Committee's Guidelines and Regulations for Animal Care.

ISOLATION AND CULTURE OF RAT AORTIC SMOOTH MUSCLE CELLS

Rat aortic VSMCs were isolated as previously described [Kim et al., 2012]. Under zoletil (20 mg/kg) and rompum (5 mg/kg) anesthesia, thoracic aortas from 6- to 8-week-old Sprague–Dawley rats were removed and transferred to serum-free Dulbecco's modified Eagle's medium (DMEM, Invitrogen) containing 100 U/ml of penicillin and 100 μg/ml of streptomycin. The aorta was freed from the connective tissue, and then transferred into a Petri dish containing 5 ml of an enzyme dissociation mixture containing DMEM with 1 mg/ml of collagenase type I (Sigma) and 0.5 μg/ml elastase (USB Bioscience), and incubated for 30 min at 37°C. The aorta was transferred to DMEM, and the adventitia was stripped off with forceps under a microscope. The aorta was transferred into a conical tube containing 5 ml of the enzyme dissociation mixture and incubated for 2 h at 37°C. The suspension was centrifuged at 1500 rpm for 10 min, and the pellet was resuspended in DMEM with 10% fetal bovine serum (FBS). Rat aortic vSMCs were cultured in DMEM supplemented with 10% FBS in 75 cm^2 flasks in a 37°C incubator at 5% CO_2 (Forma Scientific).

IMMUNOFLUORESCENCE

Perfused vessels were fixed overnight with 10% (v/v) neutral-buffered formaldehyde, transversely sectioned into serial thick sections, and embedded in paraffin using routine methods. Sections 2 μm thick were mounted on gelatin coated glass slides to ensure that different stains could be used on successive sections of tissue cut

through the areas of balloon injury. After deparaffinization, rehydration, and rinsing with PBS, sodium citrate antigen retrieval was performed using 10 mM sodium citrate (pH 6.0) in a microwave for 10 min. Sections were incubated in 1% H_2O_2 for 10 min to quench endogenous peroxidase. To remove flavin coenzyme auto fluorescence, tissue sections were treated with 0.1% sodium borohydride for 30 min. Samples were blocked in 2.5% normal horse serum and incubated in primary antibody (PCNA, Santa Cruz) overnight. FITC-conjugated goat anti-rabbit IgG was used as a secondary antibody. The sections were analyzed with DAPI and PCNA by confocal laser scanning microscope (LSM 700, Zeiss) and transferred to a computer equipped with ZEN2009 software. The areas are expressed as percentages of the total left ventricle. For quantification, five slices of each group were prepared and five different regions per slice were chosen for observation.

IMAGE ANALYSIS OF MITOCHONDRIAL MORPHOLOGY

To visualize the mitochondrial morphology with Mitotracker staining (Mitotracker Red CMXRos, Invitrogen), SMCs were incubated with 10% conditioned media supplemented with 200 nM Mitotracker for 30 min in 37°C incubator containing 5% CO_2 and then washed with fresh warm medium. The cells were fixed with 4% formaldehyde solution for 10 min and washed three times with PBS. Confocal laser scanning microscope (LSM 700, Zeiss) was used for visualization and the fluorescence intensity and mitochondrial morphology were analyzed using the Image J software (NIH).

MITOCHONDRIAL MORPHOMETRIC ANALYSES

Mitochondrial morphometric analysis was performed following the method of previous studies [De Vos et al., 2005]. Briefly, microscopic images were changed using Image J software (NIH) to enhance brightness and contrast for convolutions to emphasize the edges of each mitochondrial particle. After the threshold was modified, individual mitochondria were analyzed for circularity and major/minor axes. Form factor (FF: circularity value) and aspect ratio (AR: major/minor axis of an ellipse equivalent to the object) were calculated, and indicated as a scatter plot of AR versus FF in a graph for each image. Both parameters have a minimal value of 1 as a small perfect circle and the increase of value indicated as elongated mitochondria. Specifically, the value of AR is indicated mitochondrial length, and FF is indicated both mitochondrial length and branching. Approximately 200 cells were analyzed for each condition. The analyses were performed in triplicate by two individuals.

FLOW CYTOMETRY ANALYSIS

vSMCs were plated at a density of 5×10^5 cells/well in 35 mm plates and after treatments, the cells were harvested with trypsin-EDTA. The cells were washed with phosphate-buffered saline (PBS, pH 7.4) and resuspended in either saponin FACS buffers (1 × DPBS, 0.5% BSA, 0.05% Saponin, and 0.1% NaN_3). The cells were added with the primary antibody (phosphorylated-Drp-1 (Ser 616), Cell Signaling) and incubated on ice for 1 h with gently shaking. The cells were spun down at 1,300 rpm for 5 min at 4°C and washed with 300 μl of Saponin FACS buffer at 1,300 rpm for 5 min at 4°C two more times. FITC-conjugated secondary antibody was added and incubated on ice for 1 h with gentle shaking in the dark. After two more washes, flow cytometry was performed on a FACS Calibur system using CellQuest™ software (Becton Dickinson, San Jose, CA) with 10,000 events recorded for each sample. Experiments were performed three times with similar results.

CELL CYCLE

The distribution of vSMCs at different stages in the cell cycle was estimated by flow cytometry. Briefly, cells were seeded in DMEM containing 10% FBS and then starved in serum-free medium for 1 day. Cells were stimulated with H_2O_2 (1 μM) or Ang II (10 nM) for 24 h. After the treatment, cells were harvested and washed with phosphate-buffered saline (PBS; pH 7.4) and fixed with 70% ethanol diluted in PBS at 4°C. Following PBS washing, the pellet was dissolved in RNase A solution (20 μg/ml) and incubated at 37°C for 15 min. Cells were stained with propidium iodide (PI) for 30 min and analyzed using FACSVerse™ flow cytometer (BD Biosciences). The percentage of cells in each cell cycle phase was analyzed using FlowJo Version 7.5.4 software.

MEASUREMENT OF CYTOSOLIC AND MITOCHONDRIAL ROS

To measure cytosolic and mitochondrial ROS production in vSMCs, cytosolic specific staining with cytosolic (CM-H_2DCFDA) and mitochondrial specific staining with Mito Tracker Red (CM-H_2XROS) were used. vSMCs were plated at a density of 5×10^5 cells/well in 35 mm plates and the cells were harvested with trypsin-EDTA 6 h after treatments. The growth media from cells was removed and then the cells were resuspended in pre-warmed PBS containing at a final working concentration of 10 μM CM-H_2DCFDA dye for cytosolic ROS detection. The cells were incubated at 37°C for 10 min and then returned the cells to pre-warmed growth medium, followed by incubation at 37°C for 10 min to render the dye responsive to oxidation. For mitochondrial ROS detection, the cells were incubated with warmed medium containing mitoTracker Red CMXRos at 200 nM, were washed with PBS twice, and were replaced to the warmed medium containing 4% formalin. The cells were incubated at 37°C for 15 min and then washed several times with PBS. The cells were resuspended in 300 μl PBS and analyzed by FACSVerse™ flow cytometer (BD Biosciences). Data were analyzed using FlowJo Version 7.5.4 software.

TETRAMETHYLRHODAMINE METHYL ESTER (TMRM) STAINING

Mitochondrial membrane potential ($\Delta\psi_m$) was determined by using a tetramethylrhodamine methyl esters (TMRM) fluorescent dye (Invitrogen). Normal mitochondria show the accumulation of TMRM due to its positive charge. Six hours after the treatment, cells were loaded with 200 nM TMRM for 30 min at 37°C in medium. Then, the cell pellets were washed with pre-warmed with PBS and resuspended with PBS to analyze. The data were performed by FACS Aria II (Beckton Dickinson) and analyzed using FlowJo Version 7.5.4 software.

ANNEXIN V/PI APOPTOSIS ASSAY

To determine the apoptosis of cells, annexin V-FITC/PI apoptosis detection kit (BD Biosciences) was used. Briefly, cells were collected and resuspended in 200 μl medium buffer. 10 μl of annexin V

solution was added to the cell suspension and incubated for 15 min in the dark condition at room temperature. Then, 5 ul of propidium iodide (PI) were added and analyzed by flow cytometry machine. 10^4 cells were acquired on a FACSVerse™ flow cytometer (BD Biosciences) and analyzed with FlowJo, a Flow cytometry software. Annexin V-/PI- represented viable cells, Annexin V + /PI- cells represent early apoptotic cells, and PI+ cells represent necrotic or apoptotic cells.

TRANSFECTION WITH SMALL INTERFERING RNA

For small interfering RNA (siRNA) treatment, vSMCs were seeded to approximately 80% confluence. The cells were transfected using Lipofectamine 2000 (Invitrogen) with 50 nM Dlp1 siRNAs (Santa Cruz) according to the manufacturer's introduction. After 4 h of transfection, fresh DMEM containing 10% FBS was replaced and gene knockdown was assessed after 48 h using Western blotting.

WESTERN BLOTTING

The cells were washed in PBS and lysed for about 20 min with lysis buffer (Cell Signaling Technologies) containing 20 mM Tris (pH 7.5), 150 mM NaCl, 1 mM Na_2-EDTA, 1 mM EGTA, 1% Triton, 2.5 mM sodium pyrophosphate, 1 mM β-glycerophosphate, 1 mM Na_3VO_4, 1 mg/ml leupeptin, and 1 mM phenylmethylsulfonyl fluoride. After lysates were centrifuged at 12,000 *g* for 10 min and the supernatant was retained. Protein concentrations were determined using the BCA Protein Assay Kit (Thermo Science). Proteins were separated in a sodium dodecyl sulfate-polyacrylamide gel and transferred to a polyvinylidenedi-fluoride membrane (Millipore). After blocking with Tris-buffered saline-0.1% Tween 20 (TBS-T) containing 5% nonfat dried milk for 1 h at room temperature, the membrane was washed twice with TBS-T and incubated with primary antibody (MMP2, Santa Cruz; MMP9, Abcam; p-PKC, Cell Signaling; PKC, Cell Signaling; p-MEK, Cell Signaling; MEK, Cell Signaling; p-ERK, Santa Cruz; ERK, Cell Signaling; p-Dlp1 (ser 616), Cell Signaling; Dlp1, BD Biosciences; NOX1, Sigma–Aldrich; NOX4, Abcam and β-actin, Abcam) overnight at 4°C. The membrane was washed three times with TBS-T for 10 min and then incubated for 1 h at room temperature with horseradish peroxidase-conjugated secondary antibodies. The bands were detected by an enhanced chemiluminescence (ECL) reagent (Santa Cruz Biotechnology). The band intensities were quantified using NIH Image J version 1.34e software.

RT-PCR ANALYSIS

The expression levels of various genes were analyzed by reverse transcription polymerase chain reaction (RT-PCR). Total RNA was extracted from 60 mm plates using 500 μl TRIzol® reagent (Sigma). To each sample, 100 μl chloroform was added and vortexed for approximately 10 s. The samples were then centrifuged at 12,000 rpm at 4°C for 15 min. Of the three resulting layers, the upper transparent layer was collected in a new tube. Thereafter, 300 μl 2-propanol was added to the sample, and the mixture was inverted for approximately 10 s followed by centrifugation at 12,000 rpm at 4°C for 10 min. Next, the pellet was washed with 75% ethanol mixed with diethylpyrocarbonate (DEPC; Sigma) in water. The pellet was centrifuged again at 12,000 rpm at 4°C for 5 min, and after the pellet was dried at room temperature 30 μl nuclease-free water was added. The RNA quality and quantity were determined based on the OD_{260}/OD_{280} using a DU 640 spectrophotometer (Eppendorf). Complementary DNA (cDNA) was generated with the Promega Reverse Transcription System according to the manufacturer's instructions. One microgram of total RNA was reverse-transcribed in a 20 μl reaction volume containing 5 mM $MgCl_2$, 10 mM Tris-HCl (pH 9.0 at 25°C), 50 mM KCl, 0.1% Triton X-100, 1 mM dNTP mix, 20 U RNase inhibitor, 0.5 μg oligo-(dT) 15 primer, and 10 U reverse transcriptase for 15 min at 42°C. The reaction was terminated by heating at 99°C for 5 min. The PCR mix contained 10 mM of each primer, together with 200 mM Tri-HCl (pH 8.8), 100 mM KCl, 1.5 mM $MgSO_4$, 1% Triton X-100, 0.1 mM dNTP mix, and 1.25 U Taq polymerase in a total volume of 25 μl. PCR conditions consisted of denaturing at 94°C for 3 min, followed by 35 cycles of denaturation at 94°C for 30 s, annealing at 94°C for 30 s, and extension at 72°C for 30 s before a final extension at 72°C for 10 min. RT-PCR products were separated by electrophoresis on a 1.2% agarose gel (BioRad). Glyceraldehyde-3-phosphate dehydrogenase (GAPDH) was used as an internal standard, and the signal intensity of the amplified product was normalized to that of GAPDH. A Gel-Doc (BioRad) was used to visualize the bands after staining with ethidium bromide.

CELL PROLIFERATION ASSAY

vSMCs were plated in triplicate wells of 96-well plates at 2×10^3 cells per well. The cells were pretreated with DMEM containing 0.5% FBS for 48 h and then treated with Ang II (10 nM) and H_2O_2 (1 μM) for 48 h. After treatment with stimuli, cell proliferation was measured using a CCK assay kit (Dojindo). The CCK assay solution was diluted with DMEM, and then 100 μl was added to each well. After incubation for 2 h at 37°C, the absorbance was measured at 450 nm with a spectrometer.

BOYDEN CHAMBER MIGRATION ASSAY

Boyden chamber assay (Transwell cell culture chambers (NUNC)) was used to measure cell migration according to manufacturer's instruction. Cells (1×10^5 cells per well) suspended in DMEM containing 0.5% FBS were added to the upper compartment of 24-well fibronectin-coated, and 0.5% FBS DMEM was applied to the lower compartment with Ang II (10 nM) and H_2O_2 (1 μM). After incubating for 9 h at 37°C incubator maintaining 5% CO_2, the cells were fixed with 4% formaldehyde and stained with coommassie blue solution. The number of cells was counted as migrated cells in nine fields across the center and the periphery of the membrane.

WOUND-HEALING ASSAY

vSMCs were plated at a density of 3×10^5 cells/well in 6-well plates. After the cells had reached 80% confluence, cells were deprived of serum for 24 h and then incubated with mitomycin C (10 μg/mL, dissolved in culture medium), a potent inhibitor of cell proliferation, for 2 h. After incubation, the cells were wounded with 200 μl pipette tips and the starting points were marked with a marker pen at the bottom of the plates. Ang II (10 nM) and H_2O_2 (1 μM) were treated and then five randomly selected fields at the lesion border were acquired using a CCD camera (Olympus) at 0 h and 16 h. In each field, the distances from the margin of the lesion to the most migrated cells

were measured, and the mean value of the distances was taken as the mobility value of the cells in each culture dish.

AORTIC RING ASSAY

Ex vivo migrations of vSMC were measured by an aortic ring assay using Matrigel with some modifications following the protocol described by Marianne Baker et al [Baker et al., 2012]. Briefly, under zoletil (20 mg/kg) and rompum (5 mg/kg) anesthesia, the adventitia of the aortas from Sprague–Dawley rats (6 weeks) was removed enzymatically using collagenase (Sigma), and endothelia were removed by scraping the interior surfaces with forceps. After the vessels were cut as 1 mm rings and the rings were embedded in 48-well plates coated with 120 μl Matrigel (BD Biosciences), the rings were overlaid with an additional 50 μl Matrigel. The aortas were treated with PDGF-bb (20 ng/ml), 10% FBS, and Mdivi-1 (20 or 50 nM), respectively in serum-free media. Culture media were changed every 2 days with re-treatment of PDGF-bb, 10% FBS, and Mdivi-1. Using the NIH Image J version 1.34e software, digital images were taken at 6 day and 9 day for quantitative analysis of vascular SMC outgrowth.

ENZYME ACTIVITY OF MMPs

Two different methods were used to estimate the enzyme activity of MMPs. InnoZyme™ Gelatinase (MMP-2/MMP-9) Activity Assay kit (Calbiochem®) were used by manufacture's protocol, which estimates the activity of MMP2 and MMP9 simultaneously.

CAROTID ARTERY BALLOON INJURY MODEL

Balloon injury was performed as previously described [Tulis, 2007]. Briefly, under zoletil (20 mg/kg) and rompum (5 mg/kg) anesthesia, the left carotid artery was isolated and a 2-Fr Fogarty balloon catheter (Baxter Healthcare Corp.) was introduced through an external carotid arteriotomy incision, advanced to the aortic arch, inflated to produce moderate resistance, and gradually withdrawn three times. Then, the catheter was removed and the proximal external carotid artery was ligated. Sham operations were performed on the right common carotid arteries. At 7 days after balloon injury, rats were anesthetized and the carotid arteries were excised. All experimental procedures of our animal studies were approved by the Institutional Animal Care and Use Committee (IACUC, approval No. 2012–0197) at Yonsei University College of Medicine and were performed in accordance with the Committee's Guidelines and Regulations for Animal Care.

IMMUNOHISTOCHEMISTRY

Animals receiving transplants were sacrificed at 7 days after implantation, and aortas were excised from sacrificed rats and perfused with phosphate buffered saline (PBS) to remove blood and then fixed in 4% formaldehyde solution for 24 h at 4°C. Sequentially, Sections of 5-μm thicknesses were mounted onto gelatin-coated glass slides to guarantee that different stains could be used on successive tissue sections cut through the injury area. Histological analysis was performed using the manufacturer's instructions (Vector Laboratories). In brief, tissue sections were deparaffinized, rehydrated, and rinsed with PBS. Antigen retrieval was performed by microwaving for ten min with 10 mM sodium citrate (pH 6.0). Sections were incubated in 3% H_2O_2 to quench any endogenous peroxidase activity. Samples were blocked in 2.5% normal horse serum and incubated in primary antibody (α-smooth muscle actin (α-SMA), Abcam; MFN, Sigma; and p-Dlp1 (Ser 616), Cell Signaling). Biotinylated pan-specific universal secondary antibody and streptavidin/peroxidase complex reagent were used for the heart sections, which were stained with antibody using a DAB substrate kit. Counterstaining was with 1% methyl green, and dehydration progressed with 100% N-butanol, ethanol and xylene. For quantification, five slices of each group were prepared and five different regions per slice were chosen for observation.

STATISTICAL ANALYSIS

All quantified data are an average of at least triplicate samples. Error bars represent the standard errors of the mean. Comparisons between more than two groups were performed by one-way ANOVA using Bonferroni's correction. A P value less than 0.05 was considered significant.

RESULTS

ANGIOTENSIN II OR H_2O_2 INDUCE MITOCHONDRIAL FRAGMENTATION AND Drp1 Ser-616 PHOSPHORYLATION IN vSMCs

Ang II is a well-known atherosclerotic stimulus that promotes the proliferation of vSMCs via ROS production [Li et al., 2010; Valente et al., 2012]. To assess whether Ang II or H_2O_2 induced mitochondrial fission in VSMCs, MitoTracker was used to monitor mitochondrial morphology. After stimulation with Ang II or H_2O_2, mitochondria exhibited a smaller and rounder morphology compared with the elongated and branched shape of control; the ratio of fragmented mitochondria was significantly increased (Fig. 1A). Because Drp1 is the major protein that regulates mitochondrial fission, its expression and activation were assessed under the same experimental conditions. Drp1 phosphorylation at Ser-616 increased continuously for 24 h after stimulation (Fig. 1B). In contrast, total Drp1 expression was unchanged by Ang II or H_2O_2 (Supplemental Figure I). These data suggest that mitochondrial fission in response to Ang II or H_2O_2 treatment might be due to the phosphorylation of Drp1.

INHIBITION OF Drp-1 REDUCES PROLIFERATION IN vSMCs

We next tested the anti-proliferative effects of inhibiting Drp1 using Mdivi-1 [Gharanei et al., 2013] in response to Ang II or H_2O_2 stimulation. Increased cell viability and cell number were observed in vSMCs treated with Ang II. Mdivi-1 caused a dose-dependent reduction in Ang II-stimulated proliferation, whereas Mdivi-1 alone had no effect compared with control (Fig. 2A and B). Mdivi-1 also exhibited cell cycle arrest in G2/M phase (Fig. 2C). H_2O_2-induced cell proliferation was also decreased to control levels by treatment with Mdivi-1 (Supplemental Figure II). Importantly, Mdivi-1 did not induce significant cell death (data not shown). Stimulation of the angiotensin II receptor type 1 by Ang II activates various signaling pathways, including PKC and extracellular signal-regulated kinase (ERK), by enhancing ROS production [Zhang et al., 2007]. Therefore, we assessed the activation of ERK as representative signaling pathways to further assess ROS-induced proliferation [Zhang et al., 2010]. Ang II-induced ERK1/2 and its upstream kinase, MEK1/2

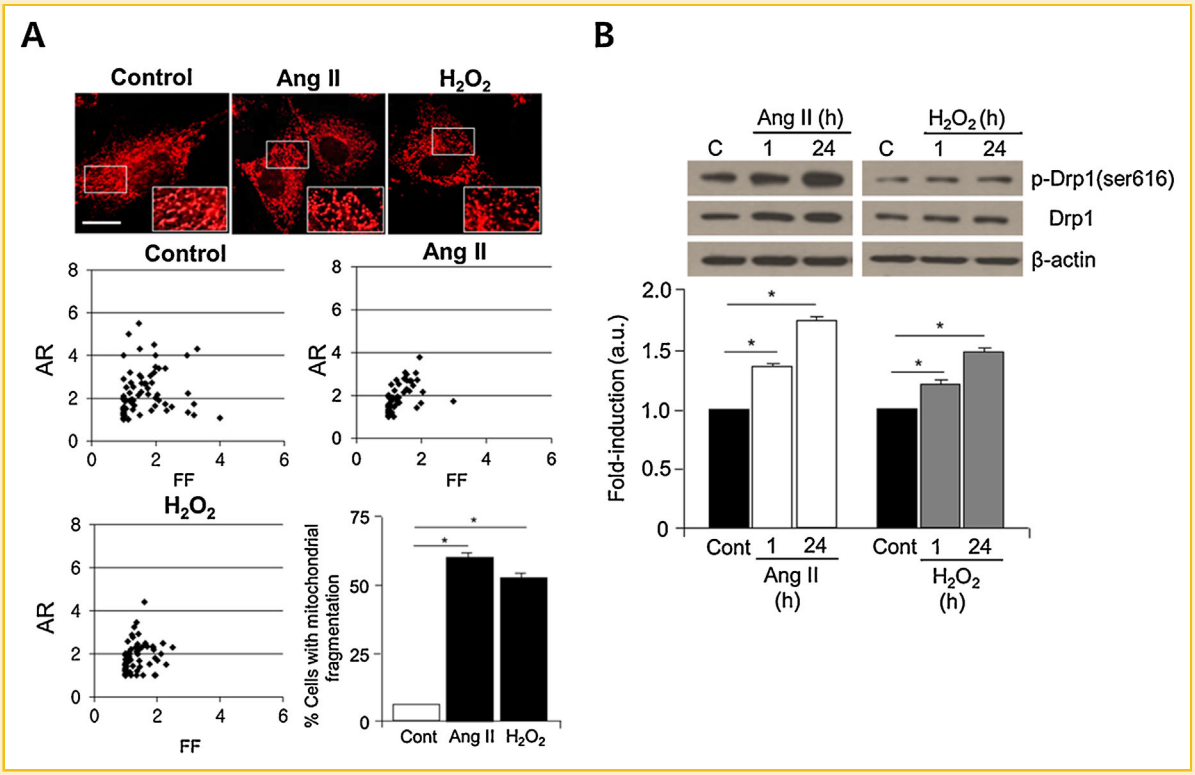

Fig. 1. Mitochondrial fission and Drp1 phosphorylation in Ang II- and H_2O_2-treated vSMCs. (A) Ang II and H_2O_2 induced mitochondrial fission in vSMCs. Cells were serum starved in media containing 0.5% fetal bovine serum for 24 h, and were then treated with 10 nM Ang II or 1 μM H_2O_2 for 24 h. Mitochondrial fission was then analyzed by staining with MitoTracker (upper panel). Mitochondrial morphology was analyzed by assessing the form factor and aspect ratio (lower panel). (B) The phosphorylation and expression level of Drp1 were assessed 1 h or 24 h after the treatment with Ang II or H_2O_2. The phosphorylation values of proteins were normalized to the total Drp1 protein. Cont, Control; Ang II, Angiotensin II; M, Mdivi-1; AR, Aspect ratio; FF, Form factor. $^*P < 0.05$.

phosphorylation were significantly inhibited by pre-treatment with Mdivi-1 (Fig. 2D). Next, the effect of Mdivi-1 on mitochondrial morphology was examined because mitochondrial fission is closely related to proliferation [Suen et al., 2008]. The form factor value and aspect ratio were close to 1 (fragmentation) after treatment with Ang II or H_2O_2, whereas Mdivi-1 restored mitochondrial morphology comparable to control (Supplemental Figure III) [Yu et al., 2008]. Because fission-mediated fragmentation is related to mitochondrial ROS production in other cell types [Yu et al., 2008], we assessed whether Mdivi-1 could inhibit Ang II-induced ROS production in vSMCs. Cytosolic and mitochondrial ROS-positive signals were significantly increased by treatment with Ang II or H_2O_2, whereas Mdivi-1 attenuated these effects (Fig. 3A and B, and Supplemental Figure IV). The ROS-mediated disruption of mitochondrial membrane potential was also restored by Mdivi-1 (Fig. 3C and Supplemental Figure V). These data suggest that Drp1 could regulate vSMC proliferation by inhibiting ROS production and MEK-ERK activation.

INHIBITION OF Drp-1 PREVENTS MIGRATION IN vSMCs

Next, migration assays were performed to analyze the anti-migration effects of Drp1. Ang II significantly induced vSMC migration in a Boyden chamber, whereas treatment with 20 μM Mdivi-1 attenuated migration (Fig. 4A). Wound-healing migration assays also showed a consistent tendency of Mdivi-1 to inhibit Ang II-stimulated migration in vSMCs (Fig. 4B). These effects of Mdivi-1 were confirmed in both assays using H_2O_2 as the ROS stimulus (Supplemental Figure VI). An aortic ring assay was performed to assess vSMC migration after stimulation with platelet-derived growth factor, which plays a role in atherogenesis [Sano et al., 2001]. Treatment with fifty micromolar Mdivi-1 caused significant reduction in migration after 9 days, confirming the in vitro data (Fig. 4C and D). To assess the signaling pathways regulated by Drp1, the expression and activity of MMPs were assessed. MMP2 and MMP9 are produced in vSMCs, and are necessary for SMC invasion [Johnson and Galis, 2004]; therefore, we investigated their expression and activity (Fig. 4E). The levels of both MMPs were increased by Ang II; however, inhibiting Drp1 down-regulated only MMP2. We further assessed MMP activity. Ang II activated both MMPs. Therefore, we may expect that the decreased activity by Mdivi-1 is mainly due to MMP2, based on the result from the protein level (Supplemental Figure VII). These results demonstrate that inhibiting Drp1 exerts anti-migration effects in the presence of atherosclerotic stimuli by regulating MMP2.

Dlp-1 INHIBITOR, Mdivi-1 PREVENTS NEOINTIMAL FORMATION IN RAT CAROTID ARTERY BALLOON INJURY MODEL

We further confirmed the anti-proliferative and -migratory effects on vSMCs using a BI model. Treatment with 50 mg/kg/day Mdivi-1 significantly reduced neointimal formation (Fig. 5). The intimal area

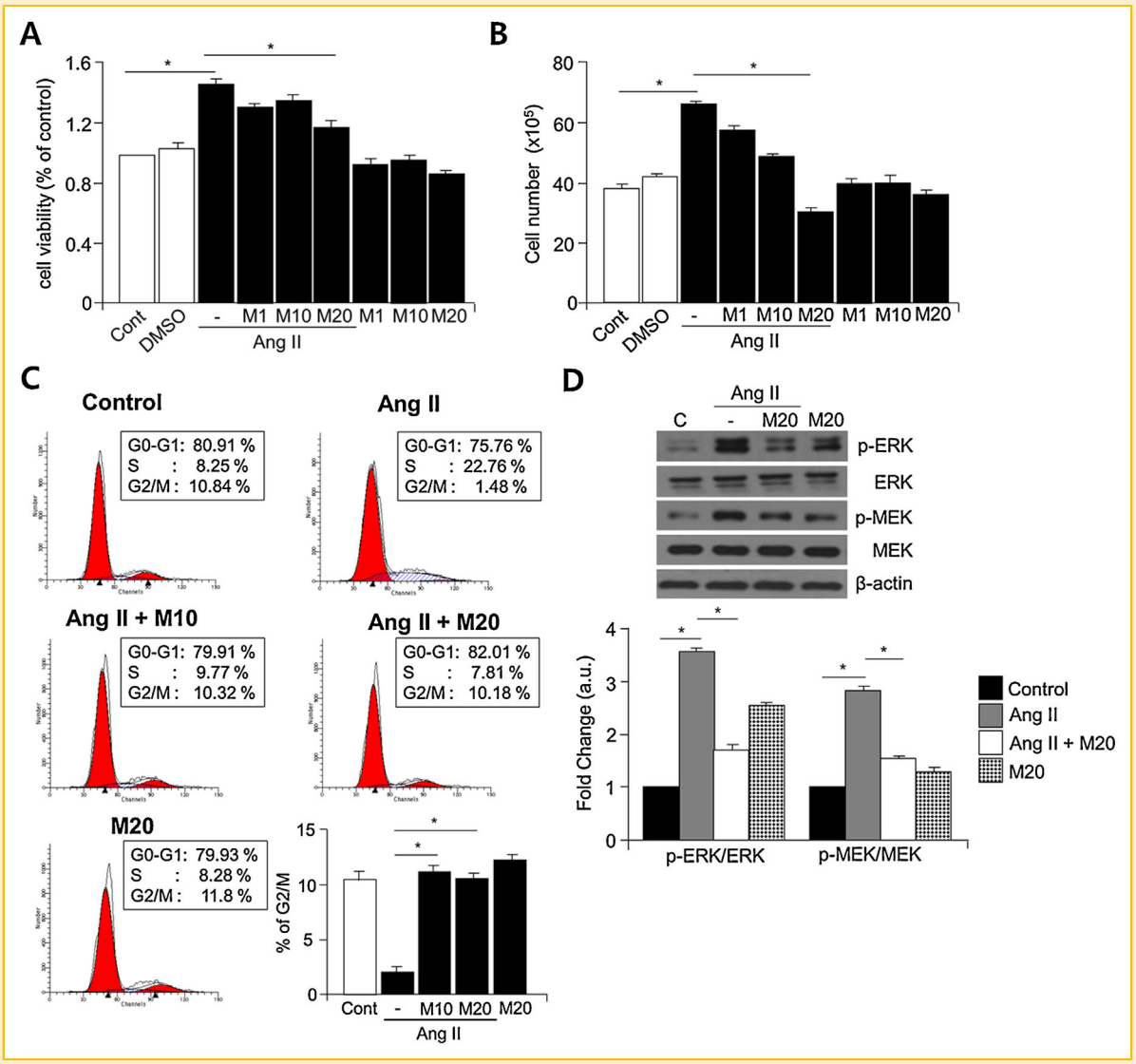

Fig. 2. Inhibiting Drp1 with Mdivi-1 suppressed Ang II-induced vSMC proliferation. (A) The proliferation of vSMCs was assessed using CCK-8 assays (B) Cell growth was analyzed using cell counting assays. Cells were serum starved in media containing 0.5% fetal bovine serum for 24 h, and then treated with 1:1000 DMSO, 10 nM Ang II, and/or 1 μM, 10 μM, or 20 μM Mdivi-1. (C) Cell cycle profiles were analyzed using flow cytometry in cells stained with propidium iodide. The data were analyzed using the ModFit LT program, and the percentage of cells in the G0/G1, S, and G2/M phases of the cell cycle are presented. (D) vSMCs were pre-treated with 20 μM Mdivi-1 for 1 h, and then stimulated with 10 nM Ang II for 10 min. The levels of ERK phosphorylation (p-ERK), total ERK, MEK phosphorylation (p-MEK), and total MEK were then evaluated by immunoblotting. Protein phosphorylation was normalized to total protein expression. Cont, Control; Ang II, Angiotensin II; M, Mdivi-1. $^{*}P < 0.05$.

and intimal area/medial area (I/M) ratio were significantly decreased compared with the BI group; however, the medial area was unchanged (Fig. 5A). Next, proliferating cell nuclear antigen (PCNA) was used as a marker to confirm vSMC proliferation in the neointimal area. The co-localization of PCNA-positive (green color) and DAPI-positive staining (blue color), indicated by arrows (yellow color), was detected in the neointimal area of the BI group (Fig. 5B). Increased vSMC-positive staining, assessed using α-smooth muscle actin, was also detected in the neointimal region (Fig. 5C). However, the carotid artery of rats injected with Mdivi-1 exhibited reduced PCNA staining (Fig. 5B) and vSMC-positive staining (Fig. 5C). In sections, the intensity of total mitofusin and Drp1 staining was comparable between the three groups (Fig. 5C). In contrast, Drp1 phosphorylation was increased in the BI group, but was decreased by Mdivi-1. These in vivo data demonstrate that Mdivi-1 could attenuate vSMC proliferation and migration during pathophysiological processes by regulating Drp1 phosphorylation.

PKCδ MAY INTERACT WITH Drp1 UNDER ATHEROSCLEROTIC STIMULUS

PKCδ enhances the proliferation, migration, and survival of mammalian cells such as vSMCs [Grossoni et al., 2007; Liu et al., 2007]; however, its exact role is controversial. The activation of PKCδ under oxidative stress was reported to translocate to the

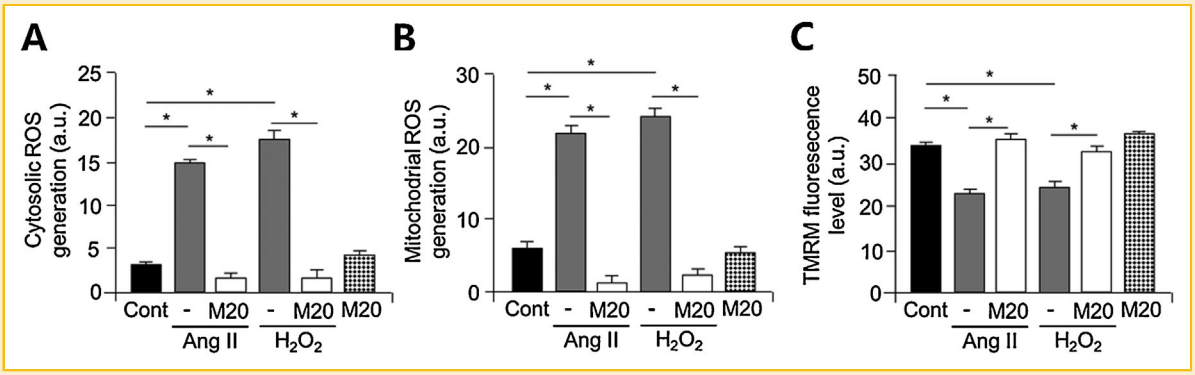

Fig. 3. H_2O_2- or Ang II-induced ROS production and mitochondrial membrane potential in Mdivi-1-treated vSMC. (A) Cytosolic ROS was stained with 10 μM CM-H_2DCFDA and (B) mitochondrial ROS was stained with 1 μM mitochondrial Red CM-H_2ROS after treatment with 10 nM Ang II, 1 μM H_2O_2 or 20 μM Mdivi-1 for 6 h after starvation in 0.5% fetal bovine serum containing media for 24 h. Cont: Control, Ang II: Angiotensin II, M: Mdivi-1. (C) A Representative FACs analysis images of TMRM fluorescence level in vSMCs treated with 10 nM Ang II, 1 μM H_2O_2 or 20 μM Mdivi-1. Cont: Control, Ang II: Angiotensin II, M: Mdivi-1. $^*P < 0.05$.

mitochondria and phosphorylate Drp1 at Ser-579/616 in neuronal cells [Qi et al., 2011]. Therefore, we hypothesized that PKCδ might activate Drp1 in vSMCs. We first assessed whether the PKCδ inhibitor rottlerin could decrease Drp1-Ser-616 phosphorylation in vSMCs using flow cytometry. Data revealed that rottlerin attenuated Drp1 activation (Supplemental Figure VIII). Surprisingly, inhibiting Drp1 using siRNA, which was confirmed by immunoblotting (Supplemental Figure IX), also reduced PKCδ phosphorylation. These data suggest that PKCδ and Drp1 reciprocally regulate each other under atherosclerotic stimuli, although we did not assess whether they physically interact.

The signaling molecules downstream of PKCδ and Drp1 are not well defined in proliferating or migrating vSMCs. We chose to analyze the activity of ERK1/2, which plays a critical role in vSMC proliferation in atherosclerotic lesions, as a representative signaling molecule [Hu et al., 2000]. ERK1/2 phosphorylation was decreased by inhibiting PKCδ (Fig. 6A) or Drp1 (Fig. 6B). Similarly, phosphorylated levels of MEK1/2, an upstream regulator of ERK1/2, were also decreased by inhibiting PKCδ or Drp1 (Fig. 6). We also analyzed MMP2 and MMP9, which are the signaling pathways related to migration. Interestingly, PKCδ regulated both MMP2 and MMP9, whereas Drp1 decreased only MMP2 protein levels, and therefore activity based on our previous observations (Fig. 4).

In summary, PKCδ and Drp1 may regulate each other as well as the MEK1/2-ERK1/2 and MMPs signaling pathways during vSMC proliferation and migration in response to the atherosclerotic stimulus Ang II (Fig. 6C).

DISCUSSION

In this study, we suggest the potential interaction between PKCδ and Drp1 in vSMCs. Subsequently, these proteins affect proliferation and migration by regulating mitochondrial fission and activating signaling molecules including MEK1/2-ERK1/2 and MMPs in response to an atherosclerotic stimulus. The Drp1 inhibitor Mdivi-1 could prevent proliferation and migration by blocking cytosolic and mitochondrial ROS production in vSMCs, and reducing aortic neointima in pathophysiological conditions such as balloon injury.

We also revealed that Ang II or H_2O_2 stimulated the phosphorylation of Drp1, but not its protein or RNA levels. In aortic sections, balloon injury significantly increased Drp1 phosphorylation at Ser-616, but not its expression. Previously, Sharp et al. investigated the expression of Drp1 in rat hearts subjected to ischemia/reperfusion (I/R) injury, which results in an environment of elevated Ca^{2+} and ROS production. Similar to the current study, they found that Drp1 protein levels were unchanged in whole cell lysates, but were significantly increased by I/R injury and decreased by Mdivi-1 in mitochondrial fractions [Sharp et al., 2014]. However, Drp1 expression in other organs or in response to different stimuli resulted in a different expression pattern. In oxygen-induced ductus arteriosus or idiopathic pulmonary arterial hypertension, ductal SMCs or pulmonary artery SMCs expressed increased Drp1 in response to mitochondrial-derived H_2O_2 or pulmonary hypertension, respectively [Marsboom et al., 2012a; Hong et al., 2013]. These data suggest that both expression and phosphorylation might be important for the effects of Drp1, depending on the pathological conditions. However, we speculate that phosphorylation is more important under the experimental conditions used in the current study, such as restenosis-prone or atherosclerotic environments.

Mdivi-1 attenuated Drp1 phosphorylation, which inhibited vSMC proliferation and migration by reducing ROS production, attenuating the activation of downstream signaling cascades, and causing cell cycle arrest. The effect of inhibiting mitochondrial fission is well established in cancer cells, but not in SMCs. In HeLa cells, Mdivi-1 exhibited G1/S or M phase cell cycle arrest and attenuated Drp1-induced Cdk1/cyclin B phosphorylation [Taguchi et al., 2007]. A recent study performed in pulmonary SMCs supports the Mdivi-1-stimulated G2/M cell cycle arrest data from the current study. In addition, the authors demonstrated that CDK1 phosphorylation plays a role in cell cycle progression and Drp1-dependent effect [Marsboom et al., 2012a]. Mdivi-1 also inhibits the expression

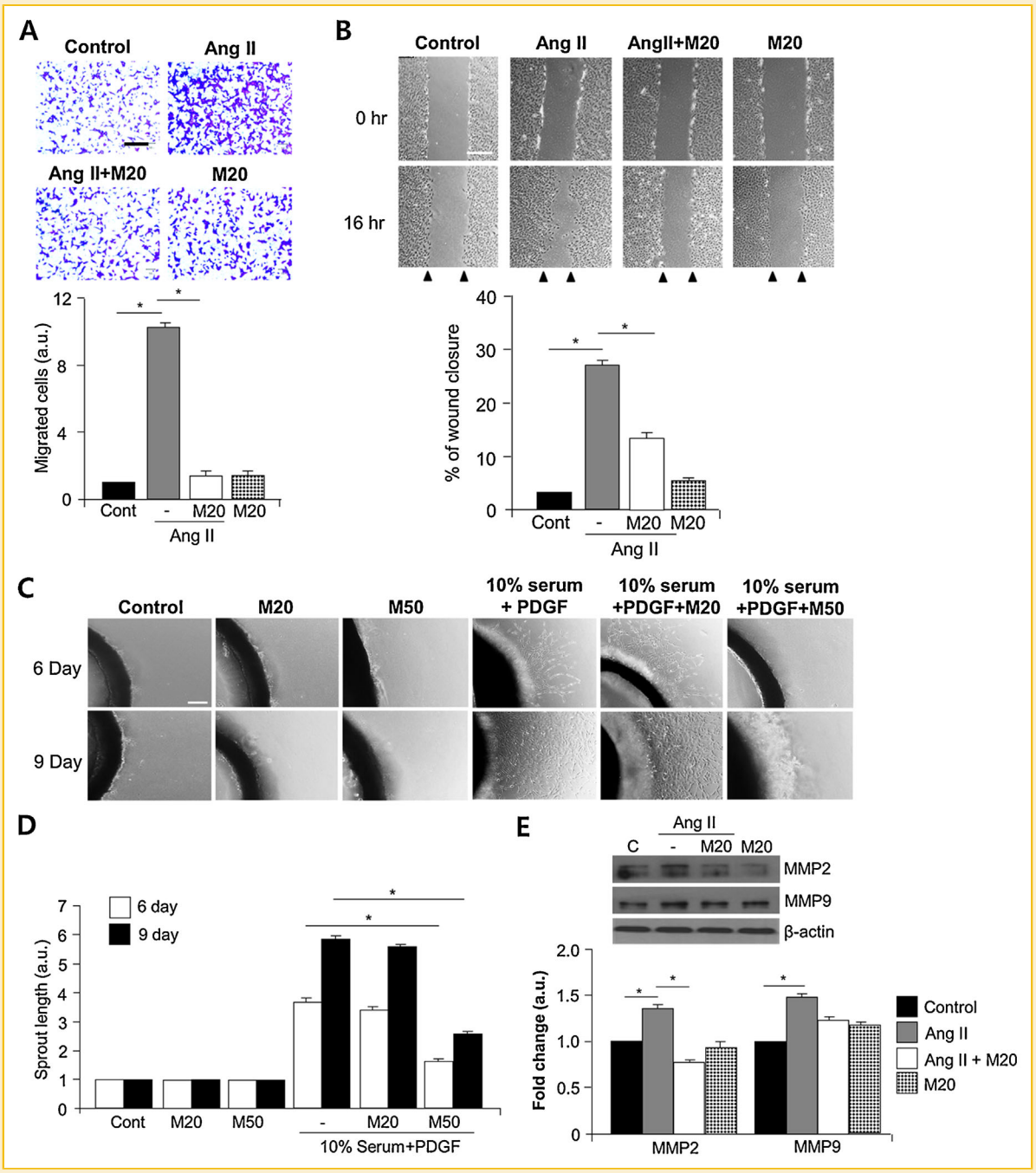

Fig. 4. Mdivi-1 suppresses vSMC migration and proliferation in vitro and ex vivo. (A) vSMCs were seeded in Boyden chambers containing 20 μM Mdivi-1 in the upper chamber, and 10 nM Ang II in the lower chamber, and were incubated for 6 h. The migrated cells were stained using Coomassie blue solution, and then counted. Black bar, 100 μm. (B) vSMCs were cultured until confluent, then scratched using a yellow pipette tip for wound healing assays, and cultured with 20 μM Mdivi-1 and 10 nM Ang II during 16 h. Upper panels show images of the wound healing assay 0 and 16 h after migration was initiated. The lower panel shows the distances that cells migrated, which were measured using Image J. White bar, 500 μm. (C) Upper panels show representative images of an aortic ring assay captured 6 and 9 days after treatment with 20 μM or 50 μM Mdivi-1, serum, and 20 ng/mL PDGF-BB. White bar, 100 μm. (D) The graph shows the cumulative length of sprouts in each group. (E) vSMCs were serum starved in media containing 0.5% fetal bovine serum for 24 h, and then treated with 10 nM Ang II for 24 h with or without 20 μM Mdivi-1. MMP2 and MMP9 protein levels were assessed by immunoblotting, and β-actin was used to normalize protein expression. Cont, Control; Ang II, Angiotensin II; M, Mdivi-1. $^{*}P < 0.05$.

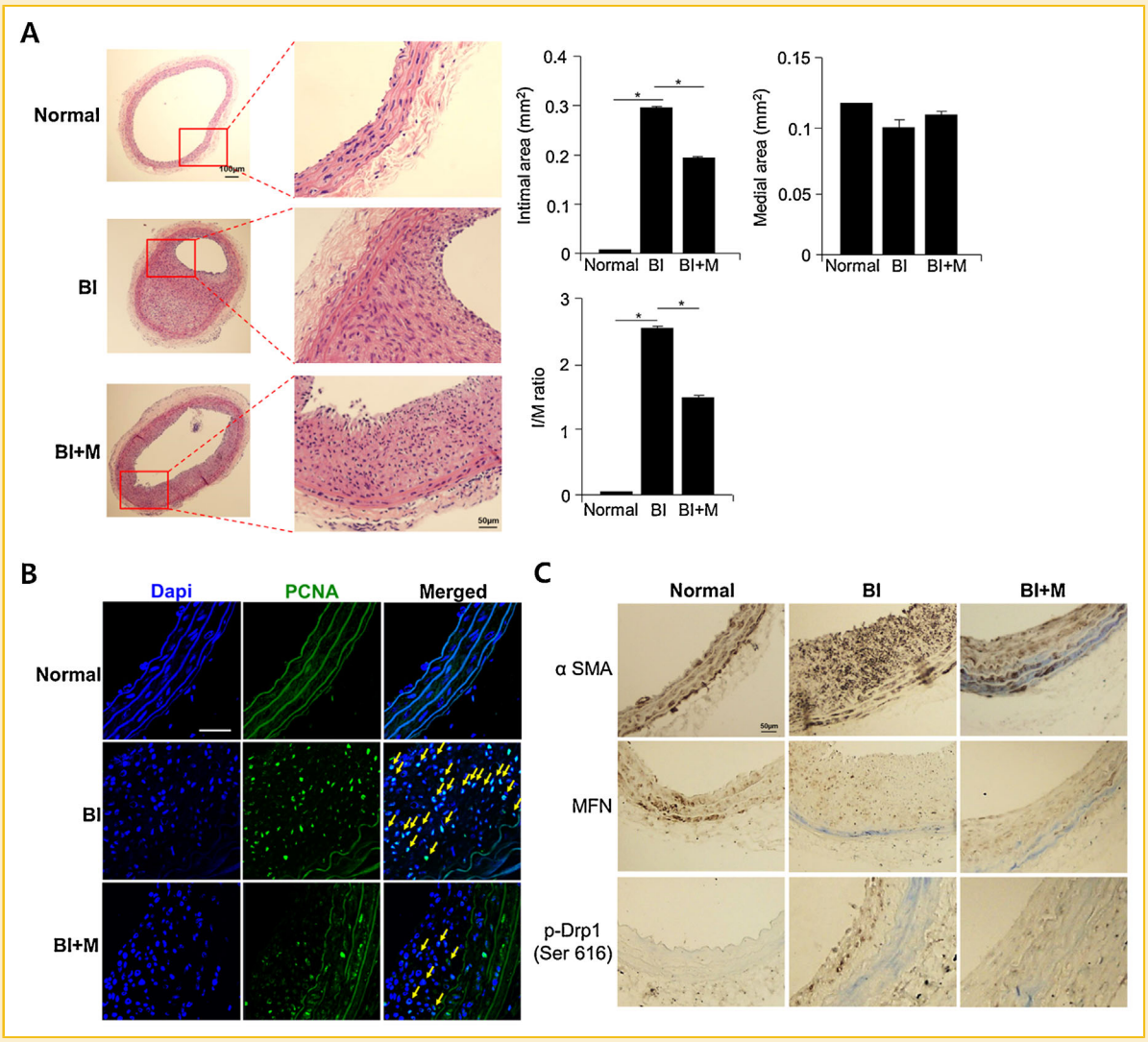

Fig. 5. Inhibitory effect of Mdivi-1 on neointimal formation in a rat carotid artery balloon injury model. (A) Hematoxylin and eosin staining of cross sections of carotid arteries from the normal, balloon-injured (BI), and balloon-injured then treated with 50 mg/kg/day Mdivi-1 groups (left panel). The intimal area, medial area, and intimal/medial area (I/M) ratio are shown in each group (right panel). Each experimental group has 5 rats. (B) Immunofluorescence staining for PCNA (green) and 4,6-diamidino-2-phenylindole (DAPI, blue) in the normal, BI, and BI-treated with Mdivi-1 groups. The yellow arrows show co-staining with PCNA and DAPI in proliferating cells. White bar, 20 μm. (C) Immunohistochemical images from the normal, BI, and BI-treated with Mdivi-1 groups after staining for alpha smooth muscle actin (α-SMA), mitofusin, and phosphorylated Drp-1 (Ser 616). N, Normal; BI, balloon injury; M, Mdivi-1. $^{*}P < 0.05$.

and activity of MMP2 in Figure 4E and Supplementary Figure VII. The evidence showing the direct relationship between Drp1 and MMP2 has not been investigated. In general, ROS is known to be closely associated with MMP2 activation as well as mitochondrial dysfunction [Lee et al., 2008]. Therefore, we may speculate that Mdivi-1 inhibited MMP2 through regulating mitochondrial dysfunction due to sustained mitochondrial fission.

We confirmed that Ang II activated PKCδ, which stimulated vSMC proliferation and migration. However, the role of PKCδ in proliferation and migration remains unclear. Several studies have suggested that the activation of PKCδ is necessary for the proliferation or migration of various types of proliferating cells [Gartsbein et al., 2006; Grossoni et al., 2007], whereas several studies also suggest its inhibitory role in proliferation [Aziz et al., 2006]. About these debates, Liu et al. [2007] suggested an interesting hypothesis that PKCδ has a dual role in vSMCs. Nevertheless, this cannot fully explain the role of PKCδ throughout restenosis or atherosclerosis, because it is relevant only when PKCδ is overexpressed ectopically. At least, inhibitory role of PKCδ might explain the SMC apoptosis that occurs in the end of atherosclerosis. The activation of STAT1 or p53 is also considered as important signaling molecules for PKCδ-mediated apoptosis [Niwa et al., 2002; DeVries et al., 2004]. However, because cell viability and proliferation were increased under the Ang II- or H_2O_2-stimulated conditions used in the current study, we did not assess STAT1 and p53 activation. More importantly, we demonstrated the reciprocal activation between

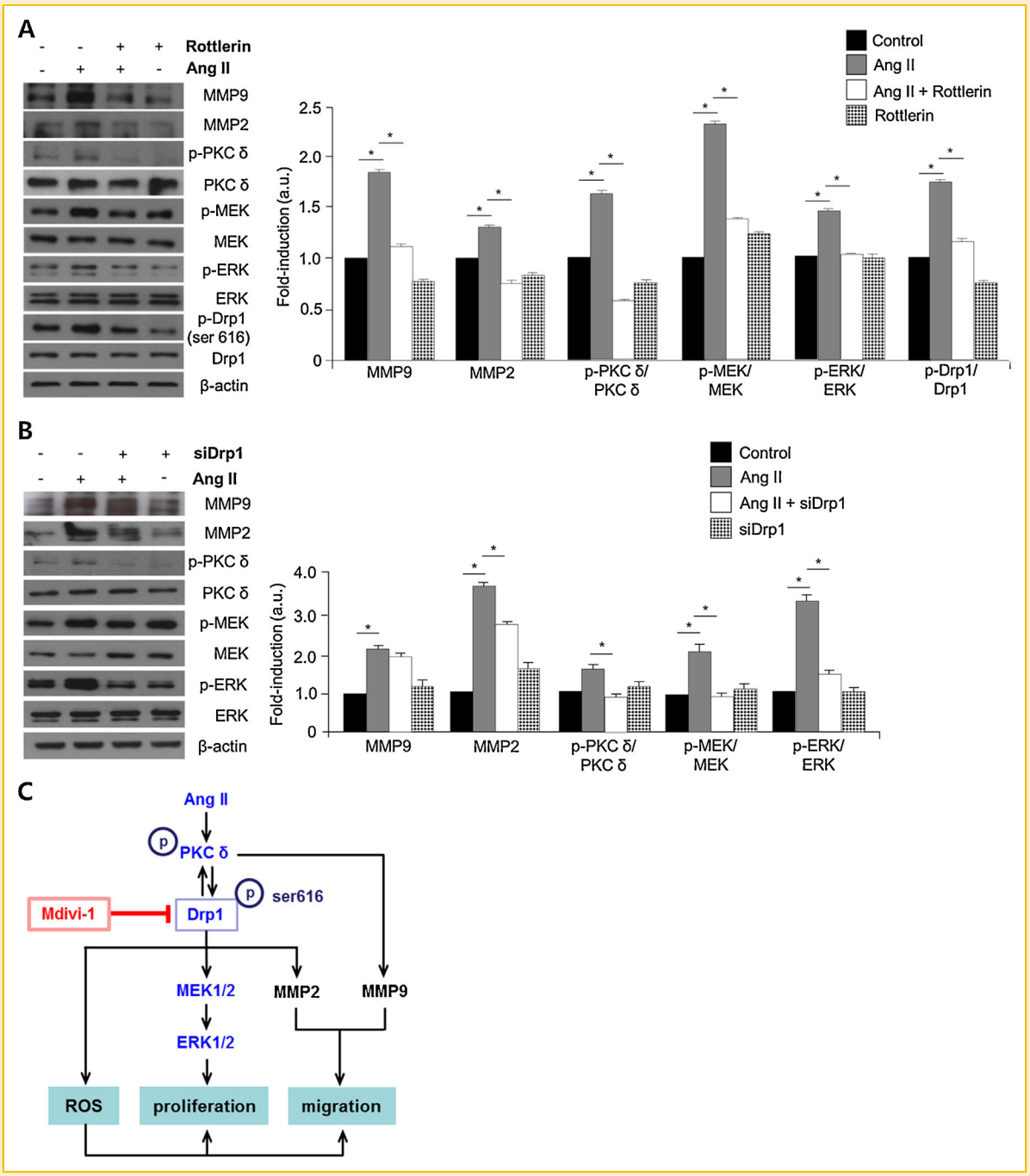

Fig. 6. Effect of a PKCδ inhibitor and Drp1 siRNA on Ang II–induced signaling pathway in vSMCs. (A) Protein lysates were harvested from vSMCs treated with10 nM Ang II with or without 1 μM rottlerin, and the total expression and phosphorylation of MMP9, MMP2, p-PKCδ, p-MEK, p-ERK, and p-Drp1 were analyzed by immunoblotting with specific antibodies. Representative immunoblots are shown (left panel). Images were quantified to demonstrate the changes in protein expression and activation (right panel). (B) Protein extracts were prepared from vSMCs transfected with siRNA-Drp1 (siDrp1) with or without treatment with 10 nM Ang II. The expression and phosphorylation of the proteins described in A were then analyzed by immunoblotting using specific antibodies. Representative immunoblots are shown (left panel). Images were quantified to demonstrate the changes in protein expression and activation (right panel). (C) The proposed Drp1 and PKCδ signaling pathways during Ang II–induced vSMC proliferation and migration. $^{*}P < 0.05$.

PKCδ and Drp1 in Ang II-stimulated vSMCs. Although this data has somewhat limited because of specificity of rottlerin and Mdivi-1 for the molecules, this finding is supported by a recent study reporting that, under conditions of oxidative stress, activated PKCδ binds to Drp1, translocates to the mitochondria, and increases mitochondrial fission in neuronal cells [Qi et al., 2011].

The current study revealed that ROS-induced SMC proliferation and migration could be prevented by Mdivi-1 in in vivo and in vitro. Mdivi-1 regulates cell proliferation and migration via PKCδ and Drp1. These results provide novel insight into the regulation of mitochondrial dynamics, which might provide a potential therapeutic approach to treat restenosis or atherosclerosis.

ACKNOWLEDGMENTS

This work was supported by grants from supported by a Korea Science and Engineering Foundation Grant funded by the Korean Government (MEST) (2014030459), a grant of the Korean Health Technology R&D Project, Ministry of Health & Welfare, Republic of Korea (A120478), a faculty research grant of the Yonsei University College of Medicine for 2013 (2013-32-0051), and a grant from the Korea Health 21 R&D Project, Ministry of Health & Welfare, Republic of Korea (HI08C2149).

REFERENCES

Aziz MH,Wheeler DL, Bhamb B, Verma AK. 2006. Protein kinase C delta overexpressing transgenic mice are resistant to chemically but not to UV radiation-induced development of squamous cell carcinomas: A possible link to specific cytokines and cyclooxygenase-2. Cancer Res 66:713–722.

Baker M, Robinson SD, Lechertier T, Barber PR, Tavora B, D'Amico G, Jones DT, Vojnovic B, Hodivala-Dilke K. 2012. Use of the mouse aortic ring assay to study angiogenesis. Nature Protocols 7:89–104.

Banai S, Wolf Y, Golomb G, Pearle A, Waltenberger J, Fishbein I, Schneider A, Gazit A, Perez L, Huber R, Lazarovichi G, Rabinovich L, Levitzki A, Gertz SD. 1998. PDGF-receptor tyrosine kinase blocker AG1295 selectively attenuates smooth muscle cell growth in vitro and reduces neointimal formation after balloon angioplasty in swine. Circulation 97:1960–1969.

Brookes PS, Yoon Y, Robotham JL, Anders MW, Sheu SS. 2004. Calcium, ATP, and ROS: A mitochondrial love-hate triangle. Am J Physiol Cell Physiol 287: C817–833.

Chalmers S, Saunter C, Wilson C, Coats P, Girkin JM, McCarron JG. 2012. Mitochondrial motility and vascular smooth muscle proliferation. Arterioscler Thromb Vasc Biol 32:3000–3011.

De Vos KJ, Allan VJ, Grierson AJ, Sheetz MP. 2005. Mitochondrial function and actin regulate dynamin-related protein 1-dependent mitochondrial fission. Current Biology 15:678–683.

DeVries TA, Kalkofen RL, Matassa AA, Reyland ME. 2004. Protein kinase Cdelta regulates apoptosis via activation of STAT1. J Biol Chem 279: 45603–45612.

Farooq V, Gogas BD, Serruys PW. 2011. Restenosis delineating the numerous causes of drug-eluting stent restenosis. Circ Cardiovasc Interv 4:195–205.

Gartsbein M, Alt A, Hashimoto K, Nakajima K, Kuroki T, Tennenbaum T. 2006. The role of protein kinase C delta activation and STAT3 Ser727 phosphorylation in insulin-induced keratinocyte proliferation. J Cell Sci 119:470–481.

Gharanei M, Hussain A, Janneh O, Maddock H. 2013. Attenuation of doxorubicin-induced cardiotoxicity by mdivi-1: A mitochondrial division/mitophagy inhibitor. PLoS ONE 8:e77713.

Givvimani S, Munjal C, Tyagi N, Sen U, Metreveli N, Tyagi SC. 2012. Mitochondrial division/mitophagy inhibitor (Mdivi) ameliorates pressure overload induced heart failure. PloS One 7:e32388.

Grossoni VC, Falbo KB, Kazanietz MG, de Kier Joffe ED, Urtreger AJ. 2007. Protein kinase C delta enhances proliferation and survival of murine mammary cells. Mol Carcinog 46:381–390.

Hehrlein C, Gollan C, Donges K, Metz J, Riessen R, Fehsenfeld P, von Hodenberg E, Kubler W. 1995. Low-dose radioactive endovascular stents prevent smooth muscle cell proliferation and neointimal hyperplasia in rabbits. Circulation 92:1570–1575.

Hong Z, Kutty S, Toth PT, Marsboom G, Hammel JM, Chamberlain C, Ryan JJ, Zhang HJ, Sharp WW, Morrow E, Trivedi K, Weir EK, Archer SL. 2013. Role of dynamin-related protein 1 (Drp1)-mediated mitochondrial fission in oxygen sensing and constriction of the ductus arteriosus. Circ Res 112:802–815.

Hu Y, Dietrich H, Metzler B, Wick G, Xu Q. 2000. Hyperexpression and activation of extracellular signal-regulated kinases (ERK1/2) in atherosclerotic lesions of cholesterol-fed rabbits. Arterioscler Thromb Vasc Biol 20:18–26.

Jandeleit-Dahm K, Burrell LM, Johnston CI, Koch KM. 1997. Elevated vascular angiotensin converting enzyme mediates increased neointima formation after balloon injury in spontaneously hypertensive rats. J Hypertens 15:643–650.

Johnson C, Galis ZS. 2004. Matrix metalloproteinase-2 and -9 differentially regulate smooth muscle cell migration and cell-mediated collagen organization. Arterioscler Thromb Vasc Biol 24:54–60.

Khan R, Agrotis A, Bobik A. 2007. Understanding the role of transforming growth factor-beta1 in intimal thickening after vascular injury. Cardiovasc Res 74:223–34.

Kim JS, Kim IK, Lee SY, Song BW, Cha MJ, Song H, Choi E, Lim S, Ham O, Jang Y, Hwang KC. 2012. Anti-proliferative effect of rosiglitazone on angiotensin II-induced vascular smooth muscle cell proliferation is mediated by the mTOR pathway. Cell Biology International 36:305–310.

Lee SJ, Seo KW, Yun MR, Bae SS, Lee WS, Hong KW, Kim CD. 2008. 4-Hydroxynonenal enhances MMP-2 production in vascular smooth muscle cells via mitochondrial ROS-mediated activation of the Akt/NF-kappaB signaling pathways. Free Radic Biol Med 45:1487–1492.

Li XC, Tong GX, Zhang Y, Liu SX, Jin QH, Chen HH, Chen P. 2010. Neferine inhibits angiotensin II-stimulated proliferation in vascular smooth muscle cells through heme oxygenase-1. Acta Pharmacologica Sinica 31:679–686.

Liu B, Ryer EJ, Kundi R, Kamiya K, Itoh H, Faries PL, Sakakibara K, Kent KC. 2007. Protein kinase C-delta regulates migration and proliferation of vascular smooth muscle cells through the extracellular signal-regulated kinase 1/2. J Vasc Surg 45:160–168.

Marsboom G, Toth PT, Ryan JJ, Hong Z, Wu X, Fang YH, Thenappan T, Piao L, Zhang HJ, Pogoriler J, Chen Y, Morrow E, Weir EK, Rehman J, Archer SL. 2012a. Dynamin-related protein 1-mediated mitochondrial mitotic fission permits hyperproliferation of vascular smooth muscle cells and offers a novel therapeutic target in pulmonary hypertension. Circ Res 110:1484–1497.

Marsboom G, Toth PT, Ryan JJ, Hong ZG, Wu XC, Fang YH, Thenappan T, Piao L, Zhang HJ, Pogoriler J, Chen YM, Morrow E, Weir EK, Rehman J, Archer SL. 2012b. Pynamin-Related Protein 1-Mediated Mitochondrial Mitotic Fission Permits Hyperproliferation of Vascular Smooth Muscle Cells and Offers a Novel Therapeutic Target in Pulmonary Hypertension. Circulation Research 110:1484–1497.

Niwa K, Inanami O, Yamamori T, Ohta T, Hamasu T, Karino T, Kuwabara M. 2002. Roles of protein kinase C delta in the accumulation of P53 and the induction of apoptosis in H2O2-treated bovine endothelial cells. Free Radic Res 36:1147–1153.

Qi X, Disatnik MH, Shen N, Sobel RA, Mochly-Rosen D. 2011. Aberrant mitochondrial fission in neurons induced by protein kinase C{delta} under oxidative stress conditions in vivo. Mol Biol Cell 22:256–265.

Rajamannan NM. 2009. Calcific aortic stenosis: Lessons learned from experimental and clinical studies. Arterioscler Thromb Vasc Biol 29:162–168.

Rehman J, Zhang HJ, Toth PT, Zhang Y, Marsboom G, Hong Z, Salgia R, Husain AN, Wietholt C, Archer SL. 2012. Inhibition of mitochondrial fission prevents cell cycle progression in lung cancer. FASEB J 26:2175–2186.

Sano H, Sudo T, Yokode M, Murayama T, Kataoka H, Takakura N, Nishikawa S, Nishikawa SI, Kita T. 2001. Functional blockade of platelet-derived growth factor receptor-beta but not of receptor-alpha prevents vascular smooth muscle cell accumulation in fibrous cap lesions in apolipoprotein E-deficient mice. Circulation 103:2955–2960.

Schieffer B, Schieffer E, Hilfiker-Kleiner D, Hilfiker A, Kovanen PT, Kaartinen M, Nussberger J, Harringer W, Drexler H. 2000. Expression of angiotensin II and interleukin 6 in human coronary atherosclerotic plaques: Potential implications for inflammation and plaque instability. Circulation 101: 1372–1378.

Schwartz SM, deBlois D, O'Brien ER. 1995. The intima. Soil for atherosclerosis and restenosis. Circ Res 77:445–465.

Seshiah PN, Weber DS, Rocic P, Valppu L, Taniyama Y, Griendling KK. 2002. Angiotensin II stimulation of NAD(P)H oxidase activity – Upstream mediators. Circ Res 91:406–413.

Sharp WW, Fang YH, Han M, Zhang HJ, Hong Z, Banathy A, Morrow E, Ryan JJ, Archer SL. 2014. Dynamin-related protein 1 (Drp1)-mediated diastolic dysfunction in myocardial ischemia-reperfusion injury: Therapeutic benefits of Drp1 inhibition to reduce mitochondrial fission. FASEB J 28:316–326.

Suen DF, Norris KL, Youle RJ. 2008. Mitochondrial dynamics and apoptosis. Genes Dev 22:1577–1590.

Taguchi N, Ishihara N, Jofuku A, Oka T, Mihara K. 2007. Mitotic phosphorylation of dynamin-related GTPase Drp1 participates in mitochondrial fission. J Biol Chem 282:11521–11529.

Tanaka H, Sukhova G, Schwartz D, Libby P. 1996. Proliferating arterial smooth muscle cells after balloon injury express TNF-alpha but not interleukin-1 or basic fibroblast growth factor. Arterioscler Thromb Vasc Biol 16:12–18.

Tulis DA. 2007. Rat carotid artery balloon injury model. Methods Mol Med 139:1–30.

Valente AJ, Yoshida T, Murthy SN, Sakamuri SS, Katsuyama M, Clark RA, Delafontaine P, Chandrasekar B. 2012. Angiotensin II enhances AT1-Nox1 binding and stimulates arterial smooth muscle cell migration and proliferation through AT1, Nox1, and interleukin-18. Am J Physiol Heart Circ Physiol 303:H282–296.

Westermann B. 2010. Mitochondrial fusion and fission in cell life and death. Nat Rev Mol Cell Biol 11:872–884.

Yamada T, Kondo T, Numaguchi Y, Tsuzuki M, Matsubara T, Manabe I, Sata M, Nagai R, Murohara T. 2007. Angiotensin II receptor blocker inhibits neointimal hyperplasia through regulation of smooth muscle-like progenitor cells. Arterioscler Thromb Vasc Biol 27:2363–2369.

Yu T, Fox RJ, Burwell LS, Yoon Y. 2005. Regulation of mitochondrial fission and apoptosis by the mitochondrial outer membrane protein hFis1. J Cell Sci 118:4141–4151.

Yu TZ, Sheu SS, Robotham JL, Yoon YS. 2008. Mitochondrial fission mediates high glucose-induced cell death through elevated production of reactive oxygen species. Cardiovasc Res 79:341–351.

Zempo N, Koyama N, Kenagy RD, Lea HJ, Clowes AW. 1996. Regulation of vascular smooth muscle cell migration and proliferation in vitro and in injured rat arteries by a synthetic matrix metalloproteinase inhibitor. Arterioscler Thromb Vasc Biol 16:28–33.

Zhang F, Hu Y, Xu Q, Ye S. 2010. Different effects of angiotensin II and angiotensin-(1–7) on vascular smooth muscle cell proliferation and migration. PLoS One 5:e12323.

Zhang GX, Lu XM, Kimura S, Nishiyama A. 2007. Role of mitochondria in angiotensin II-induced reactive oxygen species and mitogen-activated protein kinase activation. Cardiovasc Res 76:204–212.

SUPPORTING INFORMATION

Additional supporting information may be found in the online version of this article at the publisher0s web-site.